Rest-redistribution thallium-201 SPECT to detect myocardial viability.

Rest-Redistribution Thallium-201 SPECT to Detect Myocardial Viability

Roberto Sciagrà, Giovanni M. Santoro, Gianni Bisi, Paola Pedenovi, Pier Filippo Fazzini and Alberto Pupi

Nuclear Medicine Unit, Department of Clinical Physiopathology, University of Florence, and Division of Cardiology, Careggi Hospital, Florence, Italy

Rest-redistribution ^{201}Tl imaging is currently being used for myocardial viability detection, but the ideal parameters for territory classification have not yet been defined. The aim of this study was to define the optimal criteria for detecting viable myocardium and predicting postrevascularization recovery with rest-redistribution ^{201}Tl SPECT. **Methods:** In 29 patients with left ventricular dysfunction, tracer activity within asynergic segments was quantified on rest and redistribution ^{201}Tl SPECT. Viability was defined by the presence of functional recovery, which was detected by comparing wall motion in baseline and follow-up echocardiography. Discriminant function analysis and receiver operating characteristic (ROC) curve analysis were used to evaluate the relationship between ^{201}Tl data and viability. **Results:** Of 214 dysfunctioning segments (135 a-/dyskinetic), viability was demonstrated in 115 (75a-/dyskinetic). Both rest and redistribution ^{201}Tl activity in these segments were significantly higher than they were in the nonviable segments ($p < 0.0001$). Significant (>10%) reversibility was observed in 39% of the viable and in 36% of the nonviable segments ($p = 0.81$). Discriminant analysis identified redistribution activity, followed by rest activity, as the most effective predictors of functional recovery. Similar areas were found under the ROC curve for rest (0.68 ± 0.037) and for redistribution activity (0.70 ± 0.036) ($p = 0.13$). ROC curve analysis identified the optimal cutoff for redistribution activity at <60%, with 147 of 214 (69%) segments correctly classified (sensitivity = 78% and specificity = 58%). In the subset of a-/dyskinetic segments, redistribution activity presented a significantly larger ROC curve area (0.81 ± 0.038 compared to 0.77 ± 0.042, $p < 0.05$), and 103 of 135 (76%) segments were correctly classified (sensitivity = 81% and specificity = 70%). **Conclusion:** Redistribution activity is the most important parameter to be considered in rest-redistribution ^{201}Tl to differentiate viable from nonviable segments; rest activity is also valuable, whereas the meaning of reversibility appears limited. Cutoff values about 60% appear to give the most reasonable balance between sensitivity and specificity.

Key Words: hibernating myocardium; receiver operating characteristic analysis; thallium-201

J Nucl Med 1998; 39:384–390

Among the ^{201}Tl imaging protocols proposed for the detection of viable myocardium, rest-redistribution perfusion scintigraphy is considered particularly well suited when viability is the main diagnostic issue (*1–6*). Taking into account ^{201}Tl kinetics (*7,8*), hibernating myocardium, which is defined as chronically hypoperfused but viable tissue (*9*), should typically appear as a territory with reduced ^{201}Tl uptake in rest images and reversibility in the subsequent redistribution study. The equation between the rest-reversibility image pattern and hibernating myocardium, however, is disputable. First, the true incidence of significant chronic hypoperfusion in hibernating territories has been recently questioned (*10,11*). Second, the most clinically relevant feature of hibernating myocardium is its potential functional recovery after successful revascularization (*9,12,13*). The various studies that compared rest-redistribution ^{201}Tl scintigraphy with the postrevascularization functional outcome of asynergic territories indicate that not only the detection of rest defect reversibility but also the quantification of ^{201}Tl uptake are useful parameters when differentiating between hibernating and scarred myocardium (*1–6*).

Unfortunately, the different criteria for the definition of myocardial viability that have been used and the contradictory results that have been obtained make it difficult to establish the real value of rest-redistribution ^{201}Tl scintigraphy in the prediction of postrevascularization recovery. More specifically, the optimal criteria for classifying as viable and as likely to functionally improve an asynergic region on the basis of rest-redistribution ^{201}Tl data have not been systematically evaluated and are still uncertain. The purpose of this study was, therefore, to perform a thorough analysis of the quantitative data, which can be derived from rest-redistribution ^{201}Tl SPECT, to identify the most significant parameters and the most effective positivity criteria for the detection of viable hibernating myocardium, having as a standard reference the presence of postrevascularization recovery of regional function.

MATERIALS AND METHODS

Patient Population

The study population consisted of 29 patients who fulfilled the following admission criteria: previous (>3 mo before the start of the study) myocardial infarction, depressed left ventricular function [left ventricular ejection fraction (LVEF) of <50%] with severe regional wall motion abnormality and scheduled revascularization procedure. There were 27 men and 2 women with an overall mean age of 60.3 ± 9.1 yr. None had recent (<3 mo before the start of the study) unstable angina, heart disease [other than coronary artery disease (CAD)], or history of prior revascularization procedures. The decision to submit the patients to revascularization was taken by the referring cardiologist and was not based on the results of the present protocol. In particular, history of low-level effort angina and/or dyspnea, angiographic evidence of multivessel CAD and detection of contractile reserve using low-dose dobutamine echocardiography were the main criteria that guided the referring cardiologist's decision.

Study Protocol

Under stable clinical conditions and without changes in medical therapy, all patients underwent, within 1 wk, two-dimensional echocardiography and rest-redistribution ^{201}Tl SPECT. Subsequently, all major epicardial coronary arteries with significant stenosis were subjected to a revascularization procedure. Perioperative infarction was excluded according to the usual clinical, electrocardiographic and enzymatic criteria. After 3 mo, in the case of coronary bypass grafting, or 1 mo, in the case of coronary angioplasty, a follow-up functional evaluation by two-dimensional echocardiography was performed. In the latter case of coronary angioplasty, restenosis had been previously excluded by a negative exercise stress test. The Ethics Committee for Human Studies of

Received Dec. 18, 1996; revision accepted May 9, 1997.

For correspondence or reprints contact: Roberto Sciagrà, MD, Nuclear Medicine Unit, Department of Clinical Physiopathology, University of Florence, Viale Morgagni 85, 50134 Florence, Italy.

our institution approved the study protocol. All patients gave their informed consent to participate in the study.

Coronary Angiography

Coronary angiography was performed using the percutaneous transfemoral technique. Percentage diameter stenosis, using multiple projections, was evaluated with the aid of calipers by two experienced observers who were unaware of patient data. Vessels showing ≥50% lumen reduction were considered diseased.

Two-Dimensional Echocardiography

Both the prerevascularization and the follow-up studies were collected using a commercially available echocardiograph (Aloka SSD-870) with 2.5- to 3.5-MHz transducers. Multiple views were obtained for each study and recorded on videotape for off-line evaluation. All studies were analyzed by two experienced observers who were blinded to the clinical and scintigraphic data and to the acquisition sequence. For the calculation of the LVEF, a monoplane area-length method was applied on three consecutive cardiac cycles examined with the apical four-chamber view, and the mean of the three measured values was used as the LVEF (*14–16*). For the analysis of regional wall motion, the left ventricle was divided into 13 segments (*17*), and wall motion and thickening of each segment were analyzed using a semiquantitative score, as follows: 1 = normal, 2 = hypokinesis, 3 = akinesis and 4 = dyskinesis (*18*). Discrepancies were resolved by consensus. For the purpose of this study, a separate analysis was also performed on segments with baseline scores of 3–4 (a−/dyskinesis). The evolution of regional wall motion in the asynergic segments was assessed by comparing the pre- and postrevascularization scores. A significant improvement was defined by a postrevascularization score decrease of ≥1 point (*6,17*). However, a change from dyskinesis to akinesis was considered insignificant (*19,20*).

Thallium-201 Scintigraphy

Patients were studied, after an overnight fast, with the injection at rest of 3 mCi (111 MBq) ^{201}Tl followed by SPECT acquisition 30 min later. The redistribution images were collected after a 3- to 4-hr delay. Both studies were acquired using an Elscint Apex SP4 gamma camera equipped with a low-energy, all-purpose collimator, with a 15% window centered on the 68- to 80-keV peak and a second 10% window centered on the 167-keV peak of ^{201}Tl. Sixty projections of 25 sec each were collected in step-and-shoot mode over a 180° arc (from the 45° right anterior oblique to the 45° left posterior oblique projection) on a 64 × 64 matrix. Filtered backprojection using a Butterworth filter with a 0.35 cutoff and an order of 5.0 was used to reconstruct the transaxial slices, which were then realigned along the heart axis.

Quantitative Analysis of SPECT Studies

Images were analyzed by two experienced observers who were blinded to all other data including the acquisition order. For the quantitative evaluation of SPECT images, the short-axis slices from the first slice with apical activity to the last slice with activity at the base were used. Their count profiles were generated by computer software and plotted onto a two-dimensional volume-weighted polar map, which was then divided into 13 segments matching echocardiographic segments. Using an automated computer procedure, average tracer activity within each segment was calculated as the total of the normalized counts of the pixels included within the segment divided by the pixel number. The segment with maximal activity was then normalized to 100, and the activity of the other segments was expressed as a percentage of the peak activity segment. The difference between redistribution and rest ^{201}Tl percentage activity (reversibility) was calculated and expressed as a percentage of the rest value. Thallium-201 uptake was defined as normal if the percentage was ≥80% (*4,6*) and as severely reduced if the percentage was <50% (*4,6*). Significant reversibility was defined as a >10% increase over the resting uptake (*4*).

Statistical Analysis

Data were expressed, as appropriate, as mean ± s.d. Receiver operating characteristic (ROC) curve areas were expressed as mean ± s.e. (*21*). Analysis of variance with the Tukey post hoc test was used for within-group (repeated measures) and between-group (classification factor = presence or absence of functional recovery) comparisons. The relationships between global and regional changes in function were assessed using the nonparametric Spearman correlation coefficient. The relationship between rest and redistribution ^{201}Tl activity was evaluated using linear regression and the Pearson's r correlation coefficient. Proportions were compared using the chi-square test with Yates' correction, as appropriate. The selection of the parameters that best differentiate viable from nonviable segments was made using discriminant function analysis. First, the significance of each parameter was analyzed using univariate discriminant analysis; then, multivariate stepwise discriminant analysis was performed. This method comprises the calculation of a linear function, including the variables that best discriminate between the groups identified by a classification factor (in this study, the presence or absence of functional recovery) and, thus, allows the assessment of the relative effect of each variable on overall discrimination (*22*). Receiver operating characteristic curves were compared using Wilcoxon statistics (*23*). A probability value of $p < 0.05$ was considered statistically significant.

RESULTS

General Findings

According to the results of coronary angiography, 55 coronary arteries were found to be affected by significant stenosis. In particular, 11 patients had one-vessel, 10 had two-vessel and 8 had three-vessel CAD. The locations of the previous myocardial infarctions were anterior in 19 patients and inferior in 10. The prerevascularization LVEF was 35% ± 6.9% (range, 23%–49%). In the baseline echocardiogram, 214 segments showed an abnormal wall motion, 79 segments being hypokinetic, 125 being akinetic and 10 being dyskinetic. A mean of 7.4 ± 2.5 segments was involved in each patient (range, 3–12). Severe regional dysfunction (a−/dyskinesis) was detected in 135 segments, with a mean of 4.7 ± 1.6 segments (range, 2–8) in each patient.

The revascularization procedure was performed by coronary artery bypass grafting in 10 patients and by percutaneous coronary angioplasty in 19 patients. In the follow-up control, the mean LVEF increased to 42.6% ± 9.3% ($p < 0.0001$). In terms of segments, 115 segments showed a significant decrease of the wall motion score and were, thus, defined as viable, whereas 99 had an unchanged wall motion abnormality and were defined as nonviable. More specifically, of the 135 a−/dyskinetic segments, 75 were viable and 60 were nonviable. On a patient basis, 25 patients had at least 1 segment with wall motion score improvement (mean, 4 ± 2.7; range, 2–10), with a mean improvement of 5 ± 3.3 points (range, 1–12). Significant correlations between LVEF increase and both number of improved segments and score decrease were observed [Spearman $\rho = 0.63$ ($p < 0.001$) and Spearman $\rho = 0.77$ ($p < 0.00001$), respectively].

Thallium-201 SPECT

In the 214 asynergic segments, the mean rest ^{201}Tl activity was 61.8% ± 18.3%, and the mean redistribution activity was 65.3% ± 20.2% (analysis of variance for repeated measures,

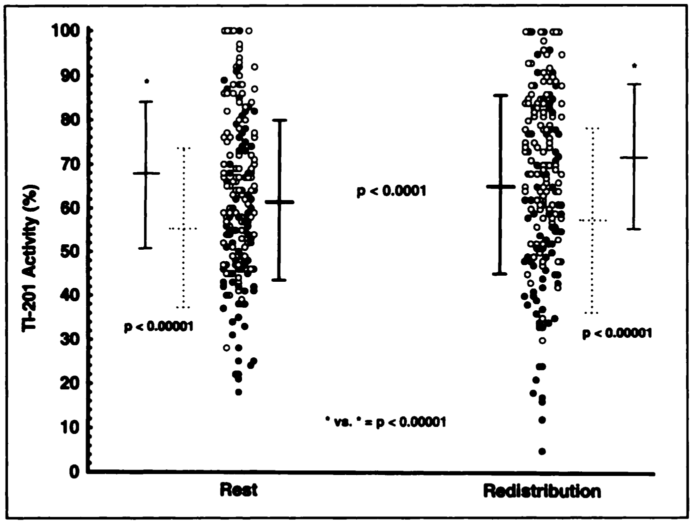

FIGURE 1. Scatterplot of rest and redistribution ^{201}Tl activity in all asynergic segments. Open circles represent viable segments and closed circles nonviable segments. The thick solid lines depict the mean ± s.d. of all segments, the thin solid lines represent the mean ± s.d. of the viable, and the dotted lines represent the mean ± s.d. of the nonviable segments.

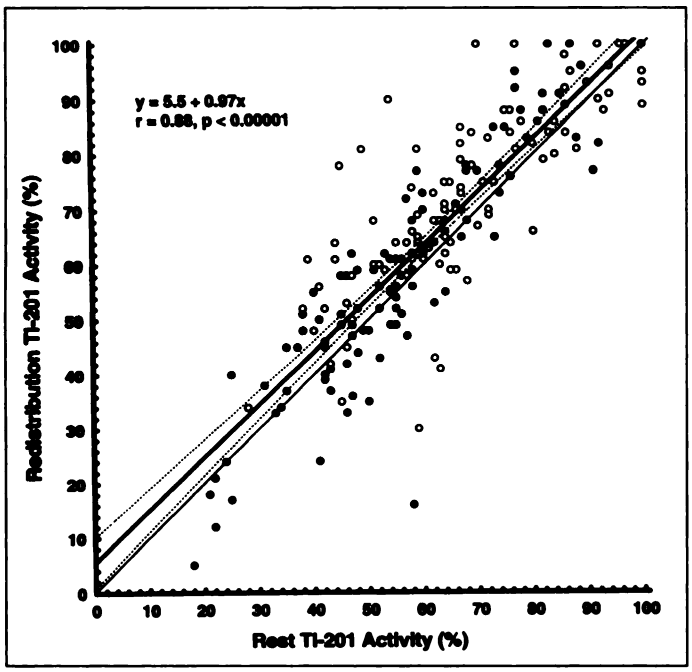

FIGURE 2. Scatterplot showing correlation of rest (x-axis) and redistribution (y-axis) ^{201}Tl activity. Open circles represent viable segments, and closed circles nonviable segments. The thin solid line indicates the identity line; the linear regression and its 95% confidence limits are depicted by the thick solid line and the thin dotted lines, respectively.

$p < 0.0001$) (Fig. 1). A highly significant correlation was observed between rest and redistribution activity ($r = 0.88$, $p < 0.00001$) (Fig. 2). The mean rest activity of the 99 nonviable segments was 55.4% ± 18%, and this value was significantly lower than that registered in the 115 viable segments (67.3% ± 16.7%, $p < 0.00001$) (Fig. 1). Similarly, the redistribution activity of the nonviable segments was significantly lower than that observed in the viable segments: 57.6% ± 21.2% compared to 72% ± 16.6% ($p < 0.00001$) (Fig. 1). The comparison between rest and redistribution images within the nonviable group did not detect any significant difference ($p = 0.12$). Conversely, a significant difference between rest and redistribution activity was registered within the viable group ($p < 0.00001$) (Fig. 1). Regarding defect reversibility, the mean value in the nonviable group was 3.2% ± 20.1% (range, −72%–60%), and in the viable group, it was 8.8% ± 18.1% (range, −34.9%–73.3%) ($p = 0.10$). The proportion of segments with >10% reversibility was 45 of 115 (39%) in the viable group and 36 of 99 (36%) in the nonviable group (chi-square = 0.6, $p = 0.81$). Only within severe uptake defects was the rate of viable segments significantly higher in reversible defects (10 of 18, 56%) than in persistent defects (8 of 38, 21%) (chi-square = 5.18, $p < 0.03$).

Table 1 shows the ^{201}Tl SPECT results in the subgroup of segments with a−/dyskinesis in the prerevascularization control. In this subgroup, a significant difference in reversibility was also observed between viable and nonviable segments ($p < 0.05$). However, the rate of segments with >10% reversibility was not significantly different between viable and nonviable segments [31 of 75 (41%) compared to 16 of 60 (27%); chi-square = 3.16, $p = 0.08$]. The proportion of segments with functional recovery was significantly higher in the presence of defect reversibility exclusively within severe defects [7 of 12 (58%) in the reversible compared to 6 of 30 (20%) in the persistent defects; chi-square = 4.24, $p < 0.05$].

Discriminant Analysis

According to univariate discriminant analysis, redistribution activity was the most significant single parameter to differentiate viable from nonviable segments both in the overall segment cohort (Table 2) and in the subset of segments with a−/dyskinesis (Table 3). The three variables (rest activity, redistribution activity and reversibility) were then submitted to multivariate stepwise discriminant analysis. Overall, only redistribution activity was selected with the adopted F-to-enter value (Table 2). Conversely, in the subset of segments with a−/dyskinesis, the two variables that were selected with the adopted F-to-enter value were redistribution activity and rest activity (Table 3).

TABLE 1
Thallium-201 Activity and Reversibility in the Segments with a−/Dyskinesis

	Rest activity (%)	Redistribution activity (%)	Reversibility (%)
All a−/dyskinetic segments (n = 135)	58.5 ± 17.5*	61.7 ± 19.9*	5.8 ± 21
Viable segments (n = 75)	66 ± 1.59†‡	71.3 ± 16.3†¶	9.7 ± 18.7‖
Nonviable segments (n = 60)	49.2 ± 14.8‡	49.8 ± 17.5¶	1 ± 22.7‖

*Rest activity vs. redistribution activity, a−/dyskinetic segments: $p < 0.001$.
†Rest activity vs. redistribution activity, viable segments: $p < 0.00005$.
‡Viable segments vs. nonviable segments, rest activity: $p < 0.00001$.
¶Viable segments vs. nonviable segments, redistribution activity: $p < 0.00001$.
‖Viable segments vs. nonviable segments, reversibility: $p < 0.05$.

TABLE 2
Results of Discriminant Analysis in All Asynergic Segments

	F	p
Univariate		
Rest activity	24.7	0.0001
Redistribution activity	30.9	0.00001
Reversibility	4.5	0.033
Stepwise		
Redistribution activity	30.9	0.00001

Receiver Operating Characteristic Analysis

Figure 3 shows the ROC curves, having as a reference the results of postrevascularization echocardiography, constructed for rest and for redistribution activity in all asynergic segments. The ROC curve areas (rest = 0.68 ± 0.037 and redistribution = 0.70 ± 0.036) were not significantly different ($p = 0.13$). The optimal cutoff point for rest ^{201}Tl was at <58%, and this allowed the correct classification of 85 of 115 (74%) viable and 58 of 99 (59%) nonviable segments. Using the most frequently adopted threshold of <50%, 96 of 115 (83%) viable and 39 of 99 (39%) nonviable segments ($p < 0.01$ compared to optimal cutoff) were correctly categorized. Conversely, the optimal cutoff point for redistribution ^{201}Tl activity was at <60%. Using this threshold, 90 of 115 (78%) viable and 57 of 99 (58%) nonviable segments were correctly identified. On the other hand, a <50% threshold in redistribution activity would have correctly classified 104 of 115 (90%) viable ($p < 0.02$ versus optimal cutoff) and 37 of 99 (38%) nonviable segments ($p < 0.005$ versus optimal cutoff). In summary, using the best cutoff value for each image set, four more segments were correctly classified by redistribution than were classified by rest ^{201}Tl activity.

Figure 4 shows the ROC curves constructed for the 135 a−/dyskinetic segments. The ROC curve area of redistribution activity (0.81 ± 0.038) was significantly larger ($p < 0.05$) than that of ^{201}Tl rest activity (0.77 ± 0.042). The sensitivity, specificity, accuracy and predictive values shown in Table 4 were obtained. In this subgroup of segments, redistribution activity using the best cutoff value allowed the correct classification of eight more segments than classification by rest activity.

DISCUSSION

Theoretically, the definition of viable myocardium would encompass each portion of tissue, including just a few viable cells. In practice, the expression viable myocardium is related to the detection of those asynergic regions that include a sufficient amount of viable cells to allow detectable functional recovery after revascularization (*9,12*). This concept implies a different

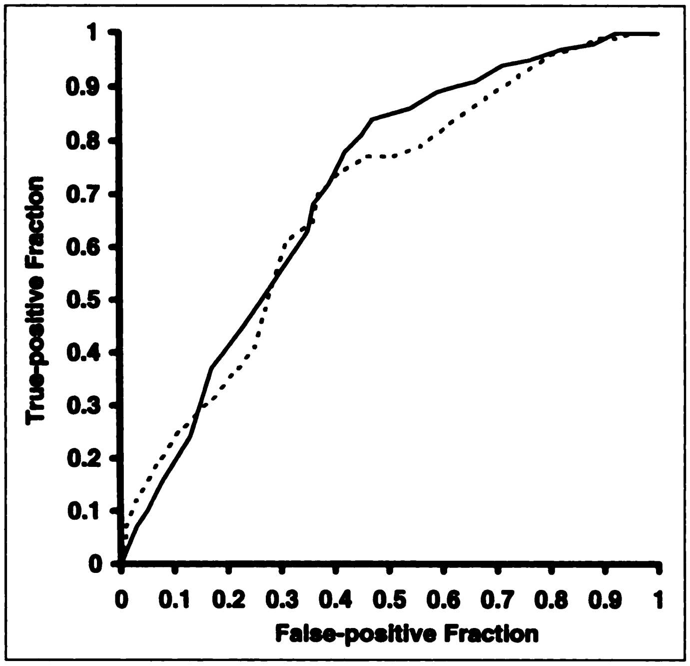

FIGURE 3. ROC curve of the diagnostic accuracy of rest (dashed line) and redistribution (solid line) ^{201}Tl activity to differentiate asynergic segments with or without postrevascularization functional recovery.

approach to viability identification than the above-mentioned broad definition. Although every technique able to recognize even the smallest amount of viable tissue would be desirable in the latter case, the prediction of functional recovery in clinically useful terms requires more selective criteria. Thus, not only a high sensitivity but also a reasonable specificity for the detection of viable myocardium likely to improve after revascularization are needed to provide valuable help in patient management and in the selection of subjects who will be submitted to the risks and costs of a revascularization procedure. Thallium-201 myocardial scintigraphy, using appropriate modifications of the standard stress-early redistribution protocol, has been considered a valuable tool for the identification of viable myocardium. Initially, major emphasis was given to the possibility of identifying tracer uptake within stress-induced perfusion defects. Accordingly, defect reversibility, obtained either by delayed redistribution imaging (*24*) or by rest-reinjection of ^{201}Tl (*25*), was considered indicative of myocardial viability. The proposal to use rest-redistribution ^{201}Tl scintigraphy as a particularly advantageous protocol for those patients in whom viability detection was the most important diagnostic issue (*1–6*) was justified by the hypothesis that, in theory, both the rest injection of the tracer and the collection of redistribution images would have been helpful to increase the possibility of

TABLE 3
Results of Discriminant Analysis in the Segments with a−/Dyskinesis

	F	p	Can corr	Chi-square	p
Univariate					
Rest activity	39.5	0.00001			
Redistribution activity	54.4	0.00001			
Reversibility	6.06	0.015			
Stepwise					
Redistribution activity	54.4	0.00001			
Rest activity	0.20	0.65			
Function	27.1	0.0001	0.54	45.5	0.00001

Can corr = canonical correlation of the discriminant function.

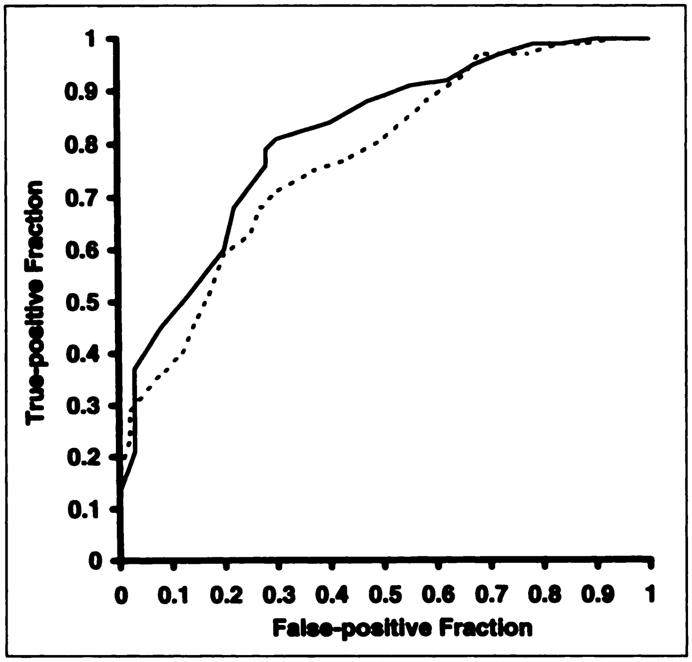

FIGURE 4. ROC curve of the diagnostic accuracy of rest (dashed line) and redistribution (solid line) ^{201}Tl activity to differentiate a−/dyskinetic segments with or without postrevascularization functional recovery.

detecting viable tissue within asynergic areas. Hibernating areas were expected to appear as rest defects with subsequent reversibility. Despite this favorable assumption, the reported reliability of the technique for the clinically useful prediction of postrevascularization recovery was erratic and rather unsatisfactory. Iskandrian et al. (*1*) divided the patients in two groups, according to the presence of normal uptake and/or defect reversibility versus presence of fixed defects, and obtained good sensitivity (80%) but a quite low specificity (60%). On the other hand, Mori et al. (*2*), who required the presence of defect reversibility to classify the asynergic regions as viable, achieved a low sensitivity (44%) but a high specificity (85%). Ragosta et al. (*3*), who evaluated tracer activity in rest and redistribution images and defect reversibility, considered the segments with ^{201}Tl uptake of <50% and no reversibility as unlikely to functionally improve after revascularization; with these criteria, the sensitivity of rest-redistribution ^{201}Tl was excellent (91%), but its specificity was very poor (31%) and the positive predictive value was unsatisfactory (57%). Udelson et al. (*4*) and Charney et al. (*5*) using SPECT imaging, and taking into account only the percentage activity in the redistribution images, reported sensitivities of 88% and 95% and specificities of 83% and 85%, respectively. However, very similar results were obtained using completely different activity thresholds to distinguish between viable and nonviable segments: 60% in the study by Udelson et al. (*4*) and 25% in the other report (*5*). Most recently, Perrone-Filardi et al. (*6*) using a < 50% cutoff point in SPECT redistribution activity obtained a 100% sensitivity but only a 22% specificity for the recognition of segments with postrevascularization recovery.

Hence, it is still unclear which parameters have to be considered and which positivity criteria have to be applied to most effectively differentiate between viable and nonviable regions in rest-redistribution ^{201}Tl scintigraphy. To this aim, in this study, the reliability for the prediction of postrevascularization recovery of the three quantitative parameters that can be derived from this protocol (rest activity, redistribution activity and reversibility) was systematically assessed using discriminant analysis to define which parameter or which combination thereof better classified the segments. Then, ROC curve analysis was applied to identify the cutoff value of the previously selected parameters that achieved the optimal balance between sensitivity and specificity.

Our results indicate that redistribution activity is the most important parameter in identification of the presence of viable myocardium. In univariate analysis, redistribution activity achieved the highest F value, followed by rest activity, whereas the F value of reversibility was only marginally significant. Within all asynergic segments, multivariate stepwise discriminant analysis selected redistribution activity alone in the discriminant function model. In the important subset of segments with a−/dyskinesis, the results of univariate discriminant analysis confirmed the superiority of redistribution activity and the very low significance of reversibility. However, rest activity also achieved a highly significant F value. Furthermore, rest activity was included in the multivariate stepwise discriminant function model, although this was achieved by accepting a relatively low F-to-enter value. The slight superiority of redistribution activity and the high informative content of resting images were confirmed by the results of ROC curve analysis. In all asynergic segments, ROC curve analysis did not demonstrate a significant superiority of redistribution over rest activity in terms of viability detection. A significant superiority of redistribution over rest activity was registered by comparing the ROC curve areas in the subset of segments with a−/dyskinesis.

Another interesting observation of this study was that the value of reversibility in ^{201}Tl rest-redistribution imaging appeared very limited. The results of discriminant analysis were confirmed by the lack of significant difference of mean reversibility between viable and nonviable segments in asynergic segments as a whole, whereas only a marginally significant difference was registered in the subset of a−/dyskinetic seg-

TABLE 4
Diagnostic Reliability of Thallium-201 Rest-Redistribution SPECT According to Receiver Operating Characteristic Analysis in the Segments with a−/Dyskinesis

	Rest activity		Redistribution activity	
Cutoff	<50%	Optimum (<59%)	<50%	Optimum (<58%)
Sensitivity	61/75 (81%)	53/75 (71%)	67/75 (89%)	61/75 (81%)
Specificity	30/60 (50%)*	42/60 (70%)*	30/60 (50%)†	42/60 (70%)†
Accuracy	91/135 (67%)	95/135 (70%)	97/135 (72%)	103/135 (76%)
Positive PV	61/91 (67%)	53/71 (75%)	67/97 (69%)	61/79 (77%)
Negative PV	30/44 (68%)	42/64 (66%)	30/38 (79%)	42/56 (75%)

*Rest activity, <50% vs. optimum (<59%): $p < 0.05$.
†Redistribution activity, <50% vs. optimum (<58%): $p < 0.01$.
PV = predictive value.

ments. Moreover, the proportion of segments with >10% reversibility was similar within the viable and the nonviable segments. Interestingly, the overall incidence of significant reversibility in our population (24%) was very close to that recently reported by Perrone-Filardi et al. (25%) (*6*). It could be argued that a quantitative threshold criterion for significant reversibility is inadequate because the same percentage change in ^{201}Tl activity might have different meaning in a segment with very depressed uptake than it would have in a region with borderline reduced activity. However, when defect reversibility was also examined in terms of segment classification changes using the common categories of normal uptake, moderate uptake defect and severe uptake defect, only reversible severe defects showed a significantly higher rate of postrevascularization recovery than the persistent severe ones, whereas no difference was registered within the moderate defects. Other reports support the opinion that the pattern of reversibility of rest defects is registered in a minority of hibernating segments. Mori et al. (*2*) found that, independent of defect reversibility, a higher rate of postrevascularization functional recovery was recorded in the patients with high ^{201}Tl activity in the redistribution images, compared with those with reduced redistribution activity. In the Italian Study on Thallium Reinjection (*26*), stress-induced defects mostly disappeared in the images obtained after a separate rest ^{201}Tl injection, with a very limited further improvement in the subsequent redistribution images and a good agreement between rest and redistribution uptake scores. On the other hand, Perrone-Filardi et al. (*20*) demonstrated a high correlation between resting ^{201}Tl uptake and rate of postrevascularization recovery. Udelson et al. (*4*) detected significant reversibility in just 17 of 98 segments with either normal or restored regional function. All these data concur in demonstrating that ^{201}Tl uptake in images acquired at least 20 min after resting injection of the tracer is already an expression of myocardial viability and that rest reversibility cannot be considered the characteristic image pattern of hibernating myocardium. The very close correlation between rest and redistribution activity that we could observe also supports these findings. Furthermore, this conclusion is in agreement with the recent PET observation that resting hypoperfusion is not necessarily present in hibernating territories (*10,11*).

After the demonstration of redistribution ^{201}Tl uptake as the most informative parameter, the second important point of this study was to identify the most effective cutoff criteria to differentiate viable from nonviable segments. In previously published studies, heterogeneous threshold values were used, and in most cases, they were arbitrarily defined. On the contrary, an attentive and systematic evaluation of the best cutoff should be performed to obtain a reasonable balance between sensitivity and specificity. On the basis of ROC curve analysis, our study suggests that the most frequently used 50% threshold is too low to achieve acceptable specificity, although sensitivity is very high. The most effective threshold appears to be about a 60% cutoff, in good agreement with the results by Udelson et al. (*4*). In the analogous subset of a−/dyskinetic segments of our population, this cutoff value achieved the same positive predictive value but a lower negative predictive value than those obtained by Udelson et al. (*4*). Therefore, our study would indicate that a cutoff value about 60% is the most effective but also that the final predictive accuracy which can be reached by rest-redistribution ^{201}Tl is probably lower than that reported by prior studies using SPECT imaging. Similar data can be derived from the recent study by Perrone-Filardi et al. (*6*).

The small patient population is a major limitation of this study, as in most other reports using postrevascularization recovery as standard reference for the definition of myocardial viability. In addition, the study cohort was necessarily selected on the basis of the decision to proceed with coronary revascularization and, thus, did not include consecutive patients with regional asynergia and left ventricular dysfunction. The spatial agreement between data obtained using echocardiography and SPECT is another important and common problem in this kind of study. Finally, we did not perform postrevascularization perfusion imaging. Therefore, the possibility of unsuccessful revascularization cannot be excluded and could be invoked to explain part of the false-positive results. This possibility, though, was limited by the attentive evaluation of the clinical and follow-up data and by the negative exercise stress testing, in the case of coronary angioplasty.

CONCLUSION

Our results indicate that the most valuable parameter for the differentiation of viable from nonviable myocardium is percentage activity in the redistribution images, whereas rest activity is useful but slightly less important. The finding of reversibility in resting defects cannot be considered of major value for the definition of myocardial viability. Focusing on the quantitative assessment of ^{201}Tl uptake in the redistribution study and using an activity threshold of 60% of peak activity can be a practically effective approach to the recognition of viable hibernating myocardium. In prospective, this would suggest that the acquisition of a single redistribution study could replace the collection of both an early and a delayed set of images, without a significant decrease in accuracy.

REFERENCES

1. Iskandrian AS, Hakki A, Kane SA, Goel IP, Mundth ED, Segal BL. Rest and redistribution thallium-201 myocardial scintigraphy to predict improvement in left ventricular function after coronary artery bypass grafting. *Am J Cardiol* 1983;51:1312–1316.
2. Mori T, Minamiji K, Kurogane H, Ogawa K, Yoshida Y. Rest-injected thallium-201 imaging for assessing viability of severe asynergic regions. *J Nucl Med* 1991;32:1718–1724.
3. Ragosta M, Beller GA, Watson DD, Kaul S, Gimple LW. Quantitative planar rest-redistribution ^{201}Tl imaging in detection of myocardial viability and prediction of improvement in left ventricular function after coronary bypass surgery in patients with severely depressed left ventricular function. *Circulation* 1993;87:1630–1641.
4. Udelson JE, Coleman PS, Metherall J, et al. Predicting recovery of severe regional ventricular dysfunction: comparison of resting scintigraphy with ^{201}Tl and ^{99m}Tc-sestamibi. *Circulation* 1994;89:2552–2561.
5. Charney R, Schwinger ME, Chun J, et al. Dobutamine echocardiography and resting-redistribution thallium-201 scintigraphy predict recovery of hibernating myocardium after coronary revascularization. *Am Heart J* 1994;128:864–869.
6. Perrone-Filardi P, Pace L, Prastaro M, et al. Assessment of myocardial viability in patients with chronic coronary artery disease. Rest-4-hour-24-hour ^{201}Tl tomography versus dobutamine echocardiography. *Circulation* 1996;94:2712–2719.
7. Weich HF, Strauss HW, Pitt B. The extraction of thallium-201 by the myocardium. *Circulation* 1977;56:188–191.
8. Pohost GM, Zir LM, Moore RH, McKusick KA, Guiney TE, Beller GA. Differentiation of transiently ischemic from infarcted myocardium by serial imaging after a single dose of thallium-201. *Circulation* 1977;55:294–302.
9. Rahimtoola SH. The hibernating myocardium. *Am Heart J* 1988;117:211–221.
10. Vanoverschelde JLJ, Wijns W, Deprè C, et al. Mechanism of chronic postischemic dysfunction in humans. New insights from the study of noninfarcted collateral-dependent myocardium. *Circulation* 1993;87:1513–1523.
11. Marinho NVS, Keogh BE, Costa DC, Lammerstma AA, Ell PJ, Camici PG. Pathophysiology of chronic left ventricular dysfunction. New insights from the measurement of absolute myocardial blood flow and glucose utilization. *Circulation* 1996;93:737–744.
12. Braunwald E, Rutherford JD. Reversible ischemic left ventricular dysfunction: evidence for the "hibernating myocardium." *J Am Coll Cardiol* 1986;8:1467–1470.
13. Rahimtoola SH. A perspective on the three large multicenter randomized clinical trials of coronary bypass surgery for chronic stable angina. *Circulation* 1985;72(suppl. V):V-123–V-135.
14. Folland ED, Parisi AF, Moynihan PF, Jones DR, Feldman CL, Tow DE. Assessment of left ventricular ejection fraction and volumes by real-time, two-dimensional echocardiography. A comparison of cineangiographic and radionuclide techniques. *Circulation* 1979;60:760–766.
15. Stamm RB, Carabello BA, Mayers DL, Martin RP. Two-dimensional echocardiographic measurement of left ventricular ejection fraction: prospective analysis of what constitutes an adequate determination. *Am Heart J* 1982;104:136–144.

16. Sciagrà R, Bisi G, Buonamici P, et al. Left ventricular cavity-to-myocardium count ratio in technetium-99m-sestamibi SPECT in the detection of patients with resting left ventricular dysfunction. *J Nucl Med* 1997;38:766–770.
17. Picano E, Marzullo P, Gigli G, et al. Identification of viable myocardium by dipyridamole-induced improvement in regional left ventricular function assessed by echocardiography in myocardial infarction and comparison with thallium scintigraphy at rest. *Am J Cardiol* 1992;70:703–710.
18. Schiller NB, Shah PM, Crawford M, et al., for the American Society of Echocardiography Committee of Standards, Subcommittee on Quantification of Two-Dimensional Echocardiography. Recommendation for quantification of the left ventricle by two-dimensional echocardiograhy. *J Am Soc Echocardiogr* 1989;5:358–367.
19. Baer FM, Voth E, Deutsch HJ, Schneider CA, Schicha H, Sechtem U. Assessment of viable myocardium by dobutamine transesophageal echocardiography and comparison with fluorine-18 fluorodeoxyglucose positron emission tomography. *J Am Coll Cardiol* 1994;24:343–353.
20. Perrone-Filardi P, Pace L, Prastaro M, et al. Dobutamine echocardiography predicts improvement of hypoperfused dysfunctional myocardium after revascularization in patients with coronary artery disease. *Circulation* 1995;91:2556–2565.
21. Hanley JA, McNeil BJ. The meaning and use of the area under a receiver operating characteristic (ROC) curve. *Radiology* 1982;143:29–36.
22. Afifi AA, Clark V. Discriminant analysis. In: *Computer-aided multivariate analysis*. New York: Von Nostrand Company; 1984:246–286.
23. Hanley JA, McNeil BJ. A method of comparing the areas under receiving operating characteristic curves derived from the same cases. *Radiology* 1983;148:839–843.
24. Kiat H, Berman DS, Maddahi J, et al. Late reversibility of tomographic myocardial thallium-201 defects: an accurate marker of myocardial viability. *J Am Coll Cardiol* 1988;12:1456–1463.
25. Dilsizian V, Rocco TP, Freedman NM, Leon MB, Bonow RO. Enhanced detection of ischemic but viable myocardium by the reinjection of thallium after stress-redistribution imaging. *N Engl J Med* 1990;323:141–146.
26. Inglese E, Brambilla M, Dondi M, et al. Assessment of myocardial viability after thallium-201 reinjection or rest-redistribution imaging: a multicenter study. *J Nucl Med* 1995;36:555–563.

Impairment of BMIPP Uptake Precedes Abnormalities in Oxygen and Glucose Metabolism in Hypertrophic Cardiomyopathy

Eiji Tadamura, Takashi Kudoh, Naoya Hattori, Masayuki Inubushi, Yasuhiro Magata, Junji Konishi, Akira Matsumori, Ryuji Nohara, Shigetake Sasayama, Muneo Yoshibayashi and Nagara Tamaki

Departments of Nuclear Medicine, Internal Medicine (Third Division) and Pediatrics, Kyoto University Faculty of Medicine, Kyoto; and Department of Nuclear Medicine, Hokkaido University School of Medicine, Sapporo, Japan

Impairment of fatty acid uptake is shown to precede myocardial perfusion abnormality using ^{123}I-labeled 15-(p-iodophenyl)-3-(R,S)-methylpentadecanoic acid (BMIPP) in an experimental model of hypertrophic cardiomyopathy (HCM) and in human studies. We have recently demonstrated that abnormalities of both glucose and oxidative metabolism precede the reduction of blood flow in HCM. The main purposes of this study were to assess the frequency of abnormal findings in FDG uptake, BMIPP uptake and oxygen metabolism and to clarify the relationship among these metabolic parameters by using PET and SPECT. **Methods:** Twenty-eight subjects with HCM underwent FDG- and acetate-PET and thallium- and BMIPP-SPECT studies at rest, respectively. After correcting for partial volume effect, real percentages of FDG and BMIPP uptake were calculated. In addition, the clearance rate constant (K mono) of acetate was measured and normalized (%) to estimate the oxygen metabolism. **Results:** There were various metabolic abnormalities observed in patients with HCM. BMIPP uptake was often impaired without significant reduction of K mono values or FDG uptake. Thus, abnormality of BMIPP uptake was more frequently observed than that for FDG uptake or K mono values ($p < 0.0001$, respectively). FDG uptake was relatively maintained even in the segments with reduced K mono values and reduced BMIPP uptake. **Conclusion:** HCM shows a variety of metabolic patterns; however, the results of our study suggest that reduction of BMIPP uptake appears to be the most sensitive indicator of metabolic abnormalities followed by reduction of oxidative metabolism in patients with HCM.

Key Words: hypertrophic cardiomyopathy; BMIPP; PET; glucose metabolism; oxidative metabolism

J Nucl Med 1998; 39:390–396

Received Jan. 16, 1997; revision accepted Apr. 15, 1997.

For correspondence or reprints contact: Eiji Tadamura, MD, Department of Nuclear Medicine and Diagnostic Imaging, Kyoto University Faculty of Medicine, 54 Shogoin Kawahara-cho, Sakyo-ku, Kyoto, 606-01, Japan.

The heart muscle can metabolize a variety of substrates including free fatty acids, glucose, lactate, pyruvate, ketone bodies and amino acids, depending on plasma substrate levels, hormonal conditions and oxygen availability (*1–4*). In the fasting state, oxidation of fatty acids is the important source of myocardial energy production. Long-chain fatty acids are known to account for approximately 70% of myocardial energy production while carbohydrates provide the majority of the remaining 30% of energy requirements (*1,3*). After carbohydrate loading, on the other hand, the myocardium utilizes glucose as a primary energy source as a result of the change in metabolic conditions. While the assessment of myocardial metabolism may be complicated by this diversity, it may lead to unique patterns of substrate utilization that reflect cardiac pathophysiology. Identification of these patterns using various metabolic tracers may contribute to our understanding of the pathophysiology in a variety of cardiac diseases (*5,6*).

Alterations in the metabolism of glucose and free fatty acid have been reported using PET and SPECT in patients with hypertrophic cardiomyopathy (HCM) (*7–12*). Sochor et al. (*7*) demonstrated inhomogeneous uptake of ^{11}C palmitate in the hypertrophic myocardium and delayed clearance from the myocardium in a small number of patients. Grover-McKay et al. (*8*) have shown the reduced uptake of FDG and free fatty acids using PET. Impaired regional fatty acid utilization has also been demonstrated using ^{123}I-labeled 15-(p-iodophenyl)–3-(R,S)-methylpentadecanoic acid (BMIPP), a radiolabeled long-chain fatty acid analog (*13,14*) in an experimental model of HCM (*9*) and in human studies (*10–12*).

Using PET, we have recently demonstrated that not only glucose but also oxidative metabolism were sometimes impaired in the hypertrophic myocardium, while the resting myocardial perfusion was not significantly changed (*15*). It is still unknown which metabolic alterations may precede the